Inorganic Chemistry

Article

pubs.acs.org/IC

Synthesis and Structural Characterization of Hydrolysis Products within the Uranyl Iminodiacetate and Malate Systems

Daniel K. Unruh, Kyle Gojdas, Erin Flores, Anna Libo, and Tori Z. Forbes*

Department of Chemistry, University of Iowa, Chemistry Building W374, Iowa City, Iowa 52242, United States

Supporting Information

ABSTRACT: The interplay of hydrolysis and chelation by organic ligands results in the formation of novel uranium species in aqueous solutions. Many of these molecular complexes have been identified by spectroscopic and potentiometric techniques, but a detailed structural understanding of these species is lacking. Identification of possible uranyl hydrolysis products in the presence of organic functional groups has been achieved by the crystallization of molecular species into a solid-state compound, followed by structural and chemical characterization of the material. The structures of three novel molecular complexes containing either iminodiacetate (*ida*) ($Na_3[(UO_2)_3(OH)_3(ida)_3]\cdot 8H_2O$ (**1**)) or malate (*mal*) ($K\text{-}(pip)_2[(UO_2)_3O(mal)_3]\cdot 6H_2O$ (**2a**) (*pip* = $C_4N_2H_{12}$), ($(pip)_3[(UO_2)_3O(mal)_3]\cdot H_2O$, and ($pi\text{-}p)_6[(UO_2)_{11}(O)_4(OH)_4(mal)_6(CO_3)_2]\cdot 23H_2O$ (**3**)) ligands have been determined by single-crystal X-ray diffraction and have been chemically characterized by IR, Raman, and NMR spectroscopies. A major structural component in compounds **1** and **2** is a trimeric 3:3 uranyl *ida* or *mal* species, but different bridging groups between the metal centers create variations in the structural topologies of the molecular units. Compound **3** contains a large polynuclear cluster with 11 U atoms, which is composed of trimeric and pentameric building units chelated by *mal* ligands and linked through hydroxyl groups and carbonate anions. The characterized compounds represent novel structural topologies for U^{6+} hydrolysis products that may be important molecular species in near-neutral aqueous systems.

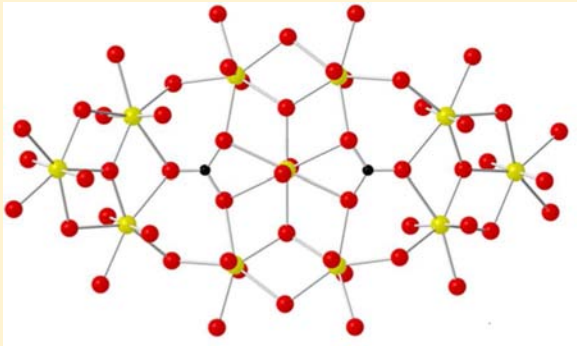

INTRODUCTION

Hydrolysis of actinide elements in aqueous solutions is important for a variety of processes associated with the nuclear fuel cycle and the transport of radionuclides in environmental systems. Aqueous actinide (An) hydroxide species are created through the general hydrolysis reaction:

$$x\mathrm{An}^{z+} + y\mathrm{OH}^- \leftrightarrow \mathrm{An}_x(\mathrm{OH})_y^{(xz-y)+1}$$

Bridging between two metal cations to form larger hydrolysis products can occur through removal of a single proton to form a shared hydroxyl group (olation) or through a two-step process that results in an oxo bridge and the release of water as a leaving group (oxolation).[1] Smaller molecular species containing two or three actinide cations generally form from hydrolysis of the metal center, but nanoscale hydrolysis products and related colloidal materials have also been observed in solution.[1,2] These larger molecular species have been identified as the potential source for fouling of chromatographic columns, hindering separation processes, and transporting sparingly soluble actinides in natural aqueous systems.[2b,3] While hydrolysis of actinides can be problematic, these polynuclear molecular species could be utilized as building units for the development of nanoscale control of advanced nuclear fuels once their structural and chemical features are well-defined.[4]

Hexavalent uranium is a naturally occurring actinide element that exists as the uranyl cation, $(UO_2)^{2+}$, in oxidizing aqueous systems and undergoes hydrolysis to form a variety of molecular species in solution and solid-state materials.[1,2] Few polynuclear hydrolysis products for U^{6+} have been identified in aqueous solutions, and a majority of these characterized species include smaller dimeric or trimeric molecules.[1] The structural characteristics of the uranyl dimer present in aqueous solutions have been investigated by experimental and theoretical methods, which indicate that the uranyl cations are coordinated to three water molecules and two bridging hydroxyl groups to form the $[(UO_2)_2(\mu_2\text{-}OH)_2(OH_2)_6]^{2+}$ moiety.[5] Eight structural configurations for the trimeric uranyl species have been proposed on the basis of spectroscopic and potentiometric data.[5] Additional experiments combining DFT calculations with results from EXAFS spectroscopy experiments have suggested that the $[(UO_2)_3(\mu_3\text{-}O)(\mu_2\text{-}OH)_3(H_2O)_6]^+$ unit is the most thermodynamically stable geometry for the trimer and is present in solutions with a pH greater than 4.[5] Similar dimeric and trimeric species are observed in the solid state, and several large uranyl hydrolysis complexes have been structurally

Received: July 3, 2013
Published: August 19, 2013

dx.doi.org/10.1021/ic401705j | *Inorg. Chem.* 2013, 52, 10191−10198

characterized, including those composed of 6 and 8 U^{6+} cations.[2a,6]

The structural features of polynuclear hydrolysis products of uranyl cations in the presence of organic functional groups are less defined, particularly for molecular complexes that are larger than dimeric units. Carboxylate functional groups strongly chelate the uranyl cation, potentially impacting the rate of hydrolysis and the structural features of the resulting polynuclear species.[7] This may be particularly important in natural aqueous systems, as Moulin et al. observed that the presence of humic matter impacts the overall speciation of uranium in aqueous solutions.[8] To explore the interplay between hydrolysis, chelation, and the structural characteristics of these species, we have begun a series of experiments investigating the molecular complexes that form at varying pH values and molar U/organic ratios. Herein, we report the synthesis and structure determination of three novel molecular uranyl hydrolysis products chelated by iminodiacetate (*ida*) or malate (*mal*) ligands: (**1**) $Na_3[(UO_2)_3(OH)_3(ida)_3]\cdot 8H_2O$, (**2a**) $K(pip)_2[(UO_2)_3O(mal)_3]\cdot 6H_2O$ (*pip* = $C_4N_2H_{12}$), (**2b**) $(pip)_3[(UO_2)_3O(mal)_3]\cdot H_2O$, and (**3**) $(pip)_6[(UO_2)_{11}(O)_4(OH)_4(mal)_6(CO_3)_2]\cdot 23H_2O$. The compounds were also characterized by vibrational and NMR spectroscopy and thermogravimetric analysis (TGA), and their potential relationships to previously identified aqueous species are discussed.

EXPERIMENTAL METHODS

Synthesis. Uranyl nitrate hexahydrate was purchased from International Bio-Analytical Industries, Inc. and purified before use due to the presence of a small amount of uranyl acetate impurities. The acetate was removed by heating the $(UO_2)(NO_3)_2\cdot 6H_2O$ in a ceramic evaporation dish until complete transformation of the material into UO_3, followed by dissolution and recrystallization of the desired product from nitric acid. All other starting reagents were used as received.

*$Na_3[(UO_2)_3(OH)_3(ida)_3]\cdot 8H_2O$ (**1**).* Compound **1** was obtained from the addition of 4 mL of a 0.2 M *ida* solution in a 50/50 mixture of water and pyridine to 1.0 mL of 0.2 M aqueous uranyl nitrate hexahydrate in a 20 mL glass scintillation vial. After mixing, an additional 1.33 mL aliquot of 1.0 M aqueous NaOH was added to bring the final pH of the solution up to 7.3. The resulting mixture was layered with 12 mL of tetrahydrofuran (THF), the vial was capped, and after 4 days, yellow, platy crystals of **1** formed. These crystals were filtered, washed with ultrapure water and ethanol, and the overall yield of the crystalline product was calculated as 70% based on U. A similar reaction in pure water also resulted in the precipitation of **1**, but yields were considerably lower (calculated yield was 6.7% based on U).

*$K(pip)_2[(UO_2)_3O(mal)_3]\cdot 6H_2O$ (**2a**) and $(pip)_3[(UO_2)_3O(mal)_3]\cdot H_2O$ (**2b**).* Crystals of **2a** were synthesized by combining 0.02 mmol uranyl nitrate and 0.02 mmol D,L-malic acid in 3 mL of ultrapure water. One milliliter of 0.2 M $K(NO_3)$ was added to the initial solution, and the pH was adjusted to 6 with 1.0 M piperazine. Liquid−liquid diffusion with THF resulted in the formation of yellow plates after 1 week in low (<2%) yields.

An alternative synthesis was developed without the addition of the K^+ cation that resulted in increased yields of the molecular species, but they produced lower quality crystals. Similar molecular species were formed in compound **2b** by combining 0.02 mmol uranyl nitrate and 0.02 mmol L-malic acid in 3 mL of ultrapure water. The pH was adjusted to 6 using 1.0 M piperazine and layered with THF in a 1:1 ratio of solvent to solution. After 1 week, yellow hexagonal plates formed on the bottom of the reaction vial with yields of up to 30% based upon U. This material was utilized for additional chemical characterization (NMR, IR, and Raman spectroscopies and TGA) of the molecular species.

*$(pip)_6[(UO_2)_{11}(O)_4(OH)_4(mal)_6(CO_3)_2]\cdot 23H_2O$ (**3**).* Compound **3** was crystallized by combining 0.02 mmol uranyl nitrate and 0.02 mmol D,L-malic acid in 3 mL of ultrapure water. The pH was adjusted to 7 using 1.0 M piperazine and layered with THF in a 2:1 ratio of solvent to solution. After 1 week, yellow-orange square plates formed on the bottom of the vial with overall yields of up to 25% based upon U.

Single-Crystal X-ray Diffraction. Crystals were taken from the mother liquor, coated in Infinium oil, and mounted on a Nonius Kappa CCD single-crystal X-ray diffractometer equipped with Mo Kα radiation (λ = 0.7107 Å) and a low-temperature cryostat set at 100 K. Data were collected with the Nonius COLLECT software package,[9] and the peak intensities were corrected for Lorentz, polarization, and background effects using the Bruker APEX II software.[10] An empirical correction for adsorption by the crystal was applied using the program SADABS. The structure solution was determined by direct methods and refined on the basis of F^2 for all unique data using the SHELXTL version 5 series of programs.[11] The U atoms were determined in each compound by direct methods, and O, C, N, and Na were identified in the difference Fourier maps calculated following refinement of the partial-structure models. Hydrogen atoms associated with organic components were constrained using a riding model, whereas the H atoms on the interstitial water molecules for **1** were determined from the difference Fourier maps following subsequent least-squares refinement of the partial-structure models.

The structural model of compound **1** was solved in the trigonal space group, *R*3*m*, with a = 16.5975(6) Å, and c = 10.6852(5) Å. A center of symmetry within the unit cell was not located for **1**, even after analysis of the data by the ADDSYM function in the PLATON software.[12] Upon completion of the structural analysis for **1**, it was determined that the crystal was merohedral twinned. A twin law (010 100 00−1) was applied with resulting structural components of 0.694 and 0.306, which reduced the R_1 value from 2.1 to 0.88%. Compound **2a** crystallizes in the monoclinic space group, *C*2/*c*, with a = 24.785(2) Å, b = 20.511(1) Å, c = 16.558(1) Å, and β = 112.60(2)°. Long-range positional disorder of the molecular species is observed due to the chiral nature of the ligand, which could not be alleviated by increasing unit cell parameters or lowering the symmetry of the space group. Twinning was also not observed, so the disorder was modeled using two positions for each U atom and free refining the occupancy of these sites to final values of 60 and 40% for the A and B sites. Additional disorder was observed for the C and O atoms of the malate ligands and modeled as split positions. The alternative synthesis method resulted in compound **2b** that crystallizes in *C*2/*c* with a = 32.02(4) Å, b = 15.91(2) Å, c = 19.86(2) Å, and β = 125.15(1)°. Identical molecular components were observed in both **2a** and **2b**, but the latter contains significantly more disorder within the crystalline lattice. Compound **3** crystallizes in the triclinic space group $P\bar{1}$ with a = 11.371(1) Å, b = 13.883(1) Å, c = 19.082(1) Å, α = 112.994(2)°, β = 93.626(2)°, and γ = 96.393(2)°. Additional information regarding the structural models for **1**, **2a**, and **3** can be found in Table 1, and crystallographic information files and tables containing selected bond lengths (Tables S2−S4) have been included in the Supporting Information (SI).

Chemical Characterization. Powder X-ray diffractograms of bulk crystalline products were collected from 5 to 60° 2θ with a step size of 0.05 and a count time of 1 s/step on a Bruker D-5000 diffractometer (Cu Kα) equipped with a LynxEye solid-state detector. After determining the purity of the samples, additional characterization (IR, Raman, and NMR spectroscopies and TGA) was performed on compounds **1**−**3**. An infrared spectrum was collected from 500 to 4000 cm^{-1} for compound **1** using a SenseIR microscope equipped with a diamond ATR tip and 100 μm aperture. Compounds **2b** and **3** were mixed with KBr, pressed into a translucent pellet, and IR spectroscopy was carried out on a Nicolet FTIR spectrometer from 500 to 4000 cm^{-1}. Raman spectroscopy was performed on single-crystal samples using a Nicolet Almega XR High Performance Dispersive spectrometer with a 785 nm excitation laser. Solid-state NMR spectra were also collected on the U/*ida* and *mal* compounds using a Bruker Avance III-500 MHz spectrometer equipped with a 4 mm double resonance magic angle spinning (MAS) probe. The MAS rate was 12 kHz, and chemical shifts were referenced on adamantane.

dx.doi.org/10.1021/ic401705j | *Inorg. Chem.* 2013, 52, 10191−10198

Table 1. Select Crystallographic Information for (1) $Na_3[(UO_2)_3(OH)_3(ida)_3]\cdot 8H_2O$, (2) $K(pip)_2[(UO_2)_3O(mal)_3]\cdot 6H_2O$, and (3) $(pip)_6[(UO_2)_{11}(O)_4(OH)_4(mal)_6(CO_3)_2]\cdot 23H_2O$

	1	2a	3
fw (g/mol)	1467.48	1542.1	4951.03
space group	*R*3*m*	*C*2/*c*	$P\bar{1}$
a (Å)	16.5975(6)	24.785(2)	11.371(1)
b (Å)	16.5975(6)	20.511(1)	13.883(1)
c (Å)	10.6852(5)	16.558(1)	19.082(1)
α (deg)	90	90	112.994(2)
β (deg)	90	112.60(2)	93.626(2)
γ (deg)	120	90	96.393(2)
V (Å^3)	2549.2(2)	7771.1(8)	2935.2(4)
*ρ*calc (g/cm^3)	2.868	2.601	2.773
μ (mm^{-1})	14.406	12.681	15.231
F(000)	2004	5552	2198
theta range (°)	3.42−25.32	1.33−25.00	1.17−25.70
data collected	$-19 < h < 19$	$-29 < h < 29$	$-13 < h < 13$
	$-19 < k < 19$	$-24 < k < 24$	$-18 < k < 18$
	$-12 < l < 12$	$-19 < l < 19$	$-23 < l < 23$
refl collect	1148	6845	11 094
GOF on F^2	1.098	1.101	1.090
final *R*	R_1 = 0.0088	R_1 = 0.0383	R_1 = 0.0462
$[I > 2\sigma(I)]$	wR_2 = 0.0230	wR_2 = 0.0486	wR_2 = 0.0632
R (all data)	R_1 = 0.0088	R_1 = 0.1049	R_1 = 0.1094
	wR_2 = 0.023	wR_2 = 0.1121	wR_2 = 0.1183

Thermogravimetric analyses of the samples were performed to determine hydration state and thermal stability of the compounds. Approximately 15−20 mg of each sample was placed onto an aluminum pan and heated from 25 to 600 °C in air at a ramp rate of 2 °C/min using a TA Instruments TGA Q500. TGA data and the powder X-ray diffraction patterns of the prepared materials can be found in the SI.

RESULTS AND DISCUSSION

Structural Descriptions. Crystallographically, **1** contains a single unique U^{6+} metal site bound by two O atoms (O2 and O3) at 1.776(3) and 1.803(3) Å with an O═U═O bond angle of 176.1(2)°, forming the well-known uranyl ion (Figure 1). The uranyl ion is further coordinated by one doubly deprotonated *ida* molecule in tridentate fashion with U−O4 and U−N1 bond lengths of 2.381(2) and 2.581(3) Å, respectively. Two OH (O1) groups further coordinate the uranyl ion at 2.305(1) Å, resulting in pentagonal bipyramidal geometry. Each isolated molecule contains three uranyl polyhedra that are bridged by μ_2-OH groups, forming a trimer with a U/*ida* ratio of 3:3. The overall charge on the trimers is 3−, which is balanced by three Na cations coordinated to seven O atoms associated with the uranyl ion, carboxylate ligand, and water molecules located in the interlayer between the trimeric species. Distances for the Na−O bonds range between 2.356(4) and 2.685(3) Å. THF was not present in the final crystal structure and appears to have only aided in the crystallization of **1**.

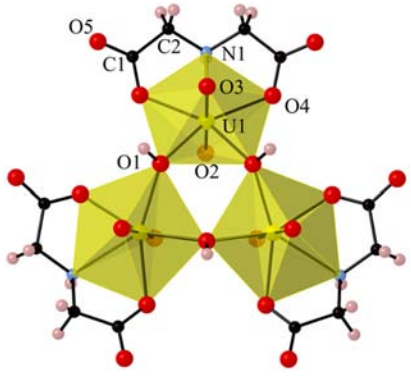

Figure 1. Polyhedral representation of **1** demonstrating the U/*ida* that contains μ_2-OH groups linking the uranyl pentagonal bipyramids into the molecular unit. Yellow polyhedra represent the U^{6+} cation, and blue, black, pink, and red spheres are N, C, H, and O atoms, respectively.

A trimeric U^{6+} *mal* complex is also observed in compounds **2a** and **2b**, but bridging between the metal centers occurs through a μ_3-O atom and the *mal* ligand, creating a different molecular topology (Figure 2). Each *mal* ligand is fully deprotonated and shared between two U^{6+} polyhedra, with the carboxylate end members bonded to separate UO_2^{2+} cations and the alcohol group bridging the metal atoms. A central μ_3-O atom is shared between three UO_2^{2+} cations resulting in a 3:3 U/*mal* molecular species. The U^{6+} polyhedra have pentagonal bipyramidal coordination with two short U−O distances with an average length of 1.79(2) Å and five longer bonds that range from 2.252(8) to 2.506(9) Å. Overall, the molecular $[(UO_2)_3O(mal)_3]^{5-}$ complex is formed, which is charge-balanced in the solid-state compound by the presence of K^+ and piperazinium cations that are located between the trimeric units. Additional water molecules are also present in the interstitial regions, leading to the overall formula of $K(pip)_2[(UO_2)_3O(mal)_3]\cdot 6H_2O$ (**2a**) or $(pip)_3[(UO_2)_3O(mal)_3]\cdot H_2O$ (**2b**).

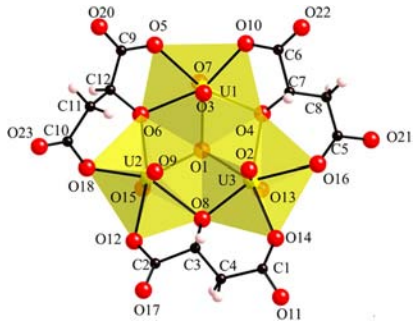

Figure 2. Trimeric unit observed in compounds **2a** and **2b**, containing one central μ_3-O atom, with the bridging malate ligands bonding to the uranyl cation.

Smaller trimeric hydrolysis products of U^{6+} have previously been isolated in the solid-state materials for both purely inorganic and hybrid organic/inorganic systems. The first trimeric species to be structurally characterized was obtained from a room temperature evaporation of a uranyl nitrate solution to form the $[(UO_2)_3(\mu_3\text{-}O)(\mu_2\text{-}OH)_3(H_2O)_6](NO_3)(H_2O)_2$ compound.[13] The molecular topology observed in this compound is identical to compound **2** as it contains a central μ_3-oxo group, although three shared μ_2-hydroxyl bridges are present in place of the *mal* ligand. Other compounds have been isolated with the same topological features, including the $[(UO_2)_3(\mu_3\text{-}O)(\mu_2\text{-}OH)_3(H_2O)_6]^+$ trimer that is linked into a three-dimensional structure through squarate ligands to form $[(UO_2)_6(C_4O_4)_3(OH)_6O_2]\cdot 9H_2O$.[14] A slightly different top-

dx.doi.org/10.1021/ic401705j | *Inorg. Chem.* 2013, 52, 10191−10198

ology is observed in $[(UO_2)_3(phen)_3(\mu_3\text{-}O)(\mu_2\text{-}OH)_2(\mu_2\text{-}NO_2)](NO_3)(DMF)_3(H_2O)$, where one of the bridging hydroxyl groups is replaced with a nitrito group to create a clover-shaped molecule.[15]

Compound **1** represents the first reported trimeric complex for the *ida* system and contains a unique structural configuration. Formation of this trimeric species likely occurs through the combination of chelation by the *ida* ligand and hydrolysis of the uranyl cation. The interplay between hydrolysis of the uranyl cation and chelation by organic ligands suggests a higher level of structural diversity for polynuclear species present in aqueous solutions than previously observed in strictly inorganic systems.[7] Organic functional groups may exert some level of control over the structural features of the polynuclear species based upon the binding constant, kinetics of the reaction, and bite angle of the chelator. The *ida* molecule coordinates to the uranyl pentagonal bipyramid in a tridentate fashion, leaving two adjacent equatorial vertices available for hydrolysis. To share a central oxo group and form $[(UO_2)_3(\mu_3\text{-}O)(\mu_2\text{-}OH)_3(H_2O)_6]^+$, individual uranyl polyhedra would need three free vertices. This can be accomplished with a ligand that chelates in a bidentate manner or bridges the metal centers, but not a tridentate coordination. Thus, other organic functional groups that bind the uranyl unit in a tridentate fashion may also favor the coordination observed in **1**.

Trimeric uranyl clusters are also present in compound **3**, but these building units are linked to a secondary molecular component to create a large cluster containing 11 U atoms (Figure 3). Ten of the uranyl cations present in the cluster are

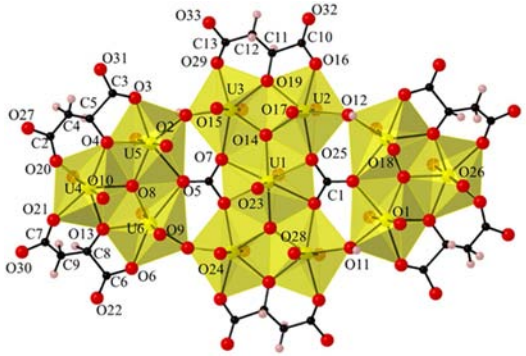

Figure 3. Two uranyl trimeric units and a pentamer are connected through bridging hydroxyl and carbonate groups to form the overall hydrolysis product present in compound **3**.

further bonded to five O atoms to form pentagonal bipyramids, but the central U^{6+} cation contains an additional O atom in the equatorial plane to create hexagonal bipyramidal coordination. Average U−O bond lengths within the uranyl cation are 1.787 Å, with distances to O atoms within the equatorial plane between 2.200(8) and 2.605(9) Å having been observed. Six *mal* ligands are bonded to the cluster, which are again shared between two U^{6+} metal centers through the deprotonated carboxylate and alcohol functional groups. The major building units on the outside of the cluster are two uranyl trimers bridged through μ_3-O and the organic ligand, with a U/*mal* ratio of 3:2. A pentameric species is located between the trimers, consisting of four U^{6+} pentagonal bipyramids and one hexagonal bipyramid. Two *mal* ligands are located on the top and bottom of the central pentamer, and these chelated uranyl dimers are bonded to the central U^{6+} hexagonal bipyramid through μ_3-O atoms and carbonate anions. The pentameric unit is linked to the two outer trimers through μ_2-OH groups and the free O atom of the carbonate anion. Carbonate was not added as a starting reagent in this synthesis, but it may be incorporated into this molecular species due to the dominance of uranyl carbonato complexes in near-neutral aqueous systems that are open to the atmosphere. Overall, the cluster has a molecular formula of $[(UO_2)_{11}(O)_4(OH)_4(mal)_6(CO_3)_2]^{12-}$ and is approximately 2 nm in diameter. Additional charge-balancing piperazinium cations and water molecules participate in hydrogen bonding to link the molecular components into a solid-state material.

Larger U^{6+} oligiomers have been observed as uranyl hydrolysis products within solid-state materials, including tetramers, hexamers, and octamers.[2a] Tetramers are the largest class of extended hydrolysis products, containing eight different topological arrangements based upon square, pentagonal, and hexagonal bipyramids.[2a] Only three compounds composed of hexameric units have been crystallized, and each contains different molecular formulas and topologies, including $[(UO_2)_6O_2]^{8+}$, $[(UO_2)_6O_2(OH)_4)]^{4+}$, and $[(UO2)_6O_2(OH)_6]^{2+}$.[6a−c] The largest uranyl hydrolysis species previously reported in the literature are the uranyl octamers, $[(UO_2)_8O_2(OH)_4]^{8+}$ and $[(UO_2)_8O_4(OH)_2]^{6+}$, which were isolated with isopthalic acid and phosphonoacetic acid.[6e,16] The $[(UO_2)_8O_2(OH)_4]^{8+}$ complex is quite unique because it was synthesized under hydrothermal conditions and contains cation−cation interactions through two uranyl oxo groups.[16] Phosphonoacetate ligands link the $[(UO_2)_8O_4(OH)_2]^{6+}$ units into a metal organic framework, and the uranyl octamer contains topological similarities to the phosphuranylite $(KCa(H_3O)_3(UO_2)[(UO_2)_3(PO_4)_2O_2]_2(H_2O)_8)$ anion topology.[6e,17]

Compound **3** also contains structural similarities to the phosphuranylite topology within the central building unit of the $[(UO_2)_{11}(O)_4(OH)_4(mal)_6(CO_3)_2]^{12-}$ cluster. The pentameric species within the cluster contains a central uranyl hexagonal bipyramid surrounded by four pentagonal bipyramids. Phosphuranylite is also composed of this building unit, but it is extended into a 1-D chain by additional edge-sharing with uranyl hexagonal bipyramids. This infinite chain of uranyl polyhedra is linked through phosphate tetrahedra to produce a 2-D sheet topology that forms a crystalline array through alkali, alkali-earth, hydronium, and uranyl cations.[17,18] Interestingly, the mineral fontanite $(Ca[(UO_2)_3(CO_3)_2O_2](H_2O)_6)$ also contains phosphuranylite anion topology, but it is linked into a 2-D sheet by edge-sharing between carbonate triangles and contains Ca^{2+} cations in the interlayers.[19]

The molecular species observed in compound **3** represents the largest isolated molecular species formed as a hydrolysis product, although other large uranyl clusters have also been isolated in the solid state, most notably the uranyl peroxide clusters.[20] These clusters possess at least one shared peroxide edge and are further linked into isolated clusters through additional bridging hydroxo groups. Many of the clusters contain fullerene topologies, including the impressive U_{60} species, which is isostructural to the carbon "buckyball" and is over 2 nm in diameter.[21] Uranyl peroxide clusters have also been constructed with additional organic linkers that also significantly change the overall structural topology of the resulting molecular species.[20,22]

Vibrational Spectroscopy. Infrared spectra obtained for compounds **1**−**3** contain a strong peak at 890 cm^{-1},

dx.doi.org/10.1021/ic401705j | *Inorg. Chem.* 2013, 52, 10191−10198

corresponding to the ν_3 antisymmetric stretching vibration for the uranyl cation (Figure 4).[23] Other major features present in

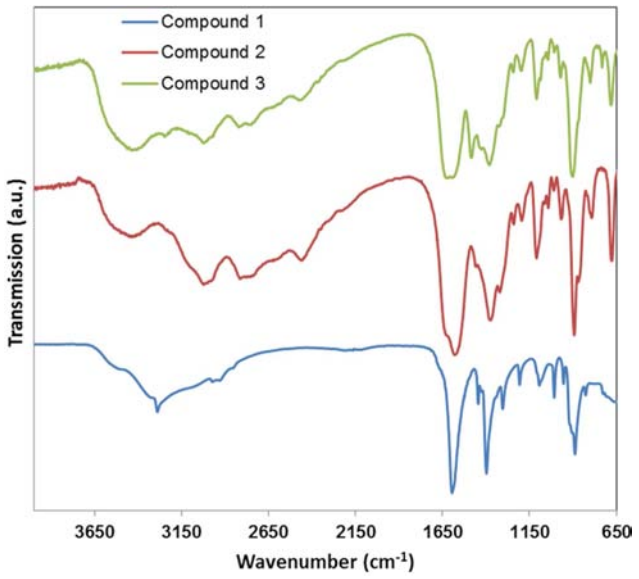

Figure 4. Infrared spectra of compounds **1**–**3**.

the spectra below 1650 cm^{-1} are associated with the *ida* and *mal* ligands, including bands between 1350 and 1400 cm^{-1} and between 1400 and 1600 cm^{-1} that can be linked to the symmetric and antisymmetric stretching vibration of the $-COO^-$ functional group.[24] The vibrational mode for the protonated carboxylate functional group is generally observed at 1700 cm^{-1} and is noticeably absent in all IR spectra, confirming that carboxylate functional groups within **1**–**3** are complexed to the uranyl cation.[24] Complexation is also confirmed by the shift in the C–N stretching vibration in **1** from approximately 1330 to 1305 cm^{-1} that occurs when the ligand is bonded to the metal center.[24]

The broad series of peaks present in the spectra from 2100 to 3600 cm^{-1} are characteristic of C–H, N–H, and O–H stretching vibrations. Bands from 2100 to 2900 cm^{-1} are associated with the symmetric and antisymmetric vibrations of the CH_2 and CH groups of the organic ligand and additional combinations. Peaks at higher wavenumbers are associated with the hydroxyl bridges and molecular water present in the interstitial regions of the crystalline lattice.[23] An additional sharp peak in **1** at 3300 cm^{-1} is associated with the N–H stretch of the central amine on the *ida* ligand.

Raman spectra for compounds **1**–**3** are dominated by the ν_1 symmetric stretching vibration of the uranyl cation, which is located at 816 cm^{-1} in all three materials (Figure 5).[23] The peak associated with the ν_1 mode for the aqueous uranyl cation, $(UO_2(H_2O)_5)^{2+}$, is generally observed at 870 cm^{-1}.[23,25] A decrease in wavenumbers for this stretching vibration in the spectra of **1**–**3** is associated with the complexation of the uranyl by organic chelators, particularly those with electron-donating properties.[25] A slight shoulder is also observed on the major peak in compounds **2** and **3**, and this band has previously been assigned to the *mal* ligand.[26] Other weaker peaks are also associated with the stretching and bending modes of the *ida* and *mal* chelators.

Weak vibrational modes associated with the carbonate anion in compound **3** are present in the IR spectra, but they cannot

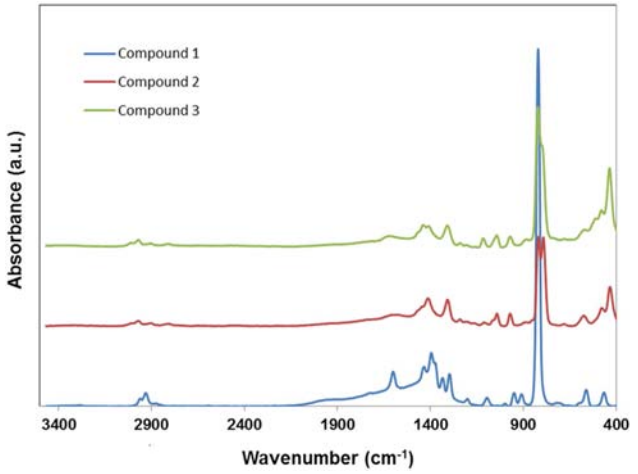

Figure 5. Raman spectra of compounds **1**–**3**.

be identified in the corresponding Raman data. Major bands associated with the planar CO_3^{3-} group include the symmetric stretching vibration (Raman active, 1115–1050 cm^{-1}), out-of plane bending (IR active, 880–835 cm^{-1}), antisymmetric stretching (IR and Raman active, 1250–1650 cm^{-1}), and the in-plane bending vibration (IR and Raman active, 670–770 cm^{-1}).[23] Two small bands at 696 and 1475 cm^{-1} are present in the IR spectra of **3** that are absent in **2** and may be indicative of the carbonate anion. No additional peaks can be identified in the Raman spectra, but the strength of the ν_1 symmetric stretching vibration of the uranyl may mask the signal.

NMR Spectroscopy. Coupled $^1H/^{13}C$ MAS NMR spectroscopy was also performed on compounds **1**–**3** to confirm the structural interpretation obtained by single-crystal X-ray diffraction. Two peaks are observed in the spectra of **1** that correspond to the C=O (185.6 ppm) and the $-CH_2$ (57.0 ppm) functional groups of the *ida* ligand (Figure 6 and Table

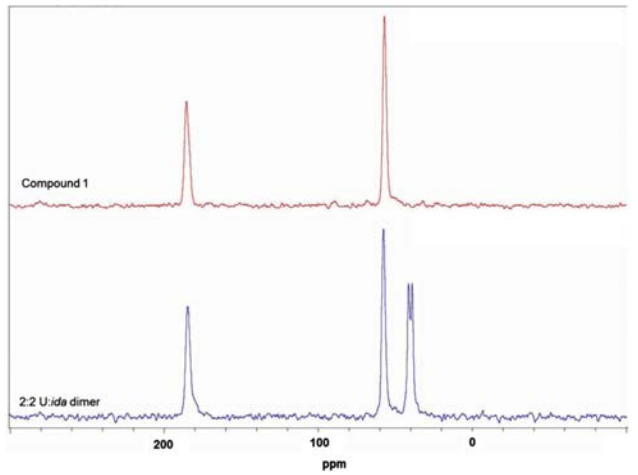

Figure 6. Coupled $^1H/^{13}C$ MAS NMR spectra of $(pip)_2[(UO_2)_2(OH)_2(ida)_2]$[27] and compound **1**.

2). Dimeric $(pip)_2[(UO_2)_2(OH)_2(ida)_2]$ was also synthesized by methods previously reported in the literature to compare to the NMR spectra of the trimeric *ida* species.[27] The NMR signals associated with the *ida* ligand are identical between the two compounds, with an additional peak at 40 ppm that corresponds to the charge-balancing piperazinium cation in the

dx.doi.org/10.1021/ic401705j | *Inorg. Chem.* 2013, 52, 10191–10198

Table 2. Coupled $^{1}H/^{13}C$ Peak Shifts (ppm) of MAS NMR for Compounds 1−3 and Related 2:2 U/*ida* Dimeric Species

compd	$-COO^{-}$	−CH	CH_2	*pip*-CH_2
1	185.6		57.0	
2:2 U/*ida* dimer	184		57.6	41.3, 38.9
2	α = 189.7	83.5	44.7	39.5
	β = 184.5			
3	α = 189.9	83.1	45.1	40.3
	β = 185.6			

dimeric material. These results highlight the difficulties in identifying hydrolysis products based upon NMR alone due to similarities in local coordination environments and the need to combine characterization techniques to gain a complete understanding of the system.

The NMR spectra of **2** and **3** are also indistinguishable because the *mal* ligand is coordinating the uranyl cation in an identical fashion (Figure 7a,b and Table 2). The high-field

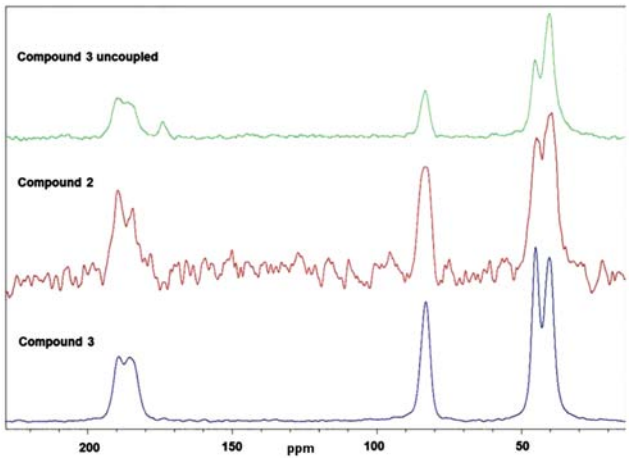

Figure 7. Coupled ^{1}H /^{13}C MAS NMR spectra of **2** and **3**.

peaks between 185 and 190 ppm are associated with the α- and β-carboxylate groups, which are shifted downfield from those observed for the uncomplexed malate ligand (178.8 and 181.6 ppm).[28] Similarly, the α-C bonded to the alcohol group has been previously documented at 71 ppm in the malate salt and is shifted to 83 ppm in both **2** and **3**, confirming the deprotonation of the alcohol group upon complexation with the uranyl cations.[28,29] The methyl groups associated with the malate ligand and piperazinium cation are located in the high-field region of the spectra between 39.5 and 45.1 ppm. Decoupling of the spectra for compound **3** reveals an additional peak at 174.0 ppm that confirms the presence of carbonate in the large clusters.[30]

Relationship to Solution Complexes. *Uranyl Iminodiacetate System.* Solutions containing U/*ida* in 1:1 and 1:2 molar ratios at a variety of pH values were previously analyzed by NMR spectroscopy (^{1}H, ^{13}C, and ^{15}N) and EXAFS experiments, with their respective stability and thermodynamic constants measured using potentiometric and calorimetric titration curves.[31] Monomeric species tend to dominate under low pH regimes with U/*ida* ratios of 1:1, whereas dimeric species are favored upon hydrolysis of the U^{6+} cation at a pH of approximately 4.3.[31a] When the *ida* concentration is increased, a mixture of 1:1 and 1:2 monomeric species is present with the 1:2 species dominating when the pH is greater than 6.

Structural studies of the U/*ida* and related U/*oda* (*oda* = digylcolic acid) systems resulted in the synthesis and characterization of 1:1 and 1:2 monomers and a 2:2 dimer.[31a,32] In addition, 1:1 and 1:2 species were also crystallized within extended chain, sheet, and framework topologies via bridging of the uranyl polyhedra through the carboxylate groups of the *ida* and *oda* molecules.[33] The syntheses of the extended structures were originally reported to occur at pH values ranging from ~1.8 to 3.2.[33a] At these lower pH values, it appears that the chelation by the *ida* and *oda* molecules is favored over the hydrolysis of uranyl ions. While the synthesis of **1** occurs at a higher U/*ida* ratio (1:4), the higher pH may increase the likelihood of forming bridging hydroxyl groups over 1:2 monomers.

The structure of **1** represents the first reported example of a trimeric species in the U/*ida* system. While the existence of a trimeric species in an aqueous solution has yet to be fully established, previous studies have eluded to its presence. One instance, in particular, where we believe a trimer molecule was present, but not identified, was in the EXAFS analysis of a 1:1 U/*ida* solution at a pH value of 4.39 conducted by Jiang et al.[31a] In this study, the authors reported a U−U distance of 4.33(5) Å, which was then compared to the dimeric $[(UO_2)_2(\mu\text{-}OH)_2(ida)_2]_2$ species that has a U−U distance of 3.85(1) Å in the solid state. The discrepancy between the two values was originally interpreted as relaxation between the OH groups of the dimer species, allowing for lengthening of the U−U distance. While some relaxation of the interatomic distances in solution can be expected, a difference in the U−U distance of 0.48 Å between solution and solid-state measurements would be quite significant. In addition, the proposed relaxation would result in the unlikely deformation of the uranyl pentagonal bipyramid due the structural constraints imposed by the tridentate *ida* molecule. As an alternative explanation, these U−U atom distances, as well as the other U−O and U−N bond distances determined by EXAFS, could be indicative of compound **1**, as the U−U bond distances are 4.311(3) Å in the solid state. Consideration for the trimeric species in solution at higher pH values could potentially alter previously reported stability and thermodynamic constants for the U/*ida* system.

Uranyl Malate System. Potentiometric, NMR, and IR spectroscopy studies on the uranyl malate system indicate that a 2:2 U/*mal* dimeric species dominates at pH values between 2 and 4.[34] This species has yet to be structurally characterized but has been predicted to contain similar bonding as observed in the trimeric system with the malate ligands bridging the two uranyl polyhedra through the deprotonated alcohol group.[29,34,35] At higher pH regions, a 3:3 U/*mal* is expected to exist, and original models depicted a square bipyramidal coordination geometry for the three uranyl groups due to steric constraints imposed by the organic ligand.[35a] Based upon structural characterization of **2** and other related structures, a uranyl pentagonal bipyramid with a shared μ_3-oxo group is the expected molecular topology in aqueous solutions.

Synthetic conditions for compounds **2** and **3** were remarkably similar, with the sole difference of 1 pH unit controlling the formation of the trimer versus the larger oligomer. Hydrolysis of the UO_2^{2+} cation begins at a pH of 4 with the formation of monomeric and dimeric hydroxyl species, and at a pH of 6, the $[(UO_2)_3(OH)_5]^{+}$ species is expected to dominate.[36] Increasing the alkalinity of the solution by 1 pH unit results in the formation of a carbanato species and may

dx.doi.org/10.1021/ic401705j | *Inorg. Chem.* 2013, 52, 10191−10198

explain the presence of the carbonate anion in the $[(UO_2)_{11}(O)_4(OH)_4(mal)_6(CO_3)_2]^{12-}$ cluster.[36a,37] Under near-neutral conditions, uranyl hydroxo carbonate species are expected to dominate, although a dimeric $[(UO_2)_2CO_3(OH)_3]^-$ species is predicted from speciation modeling of dilute solutions.[36b] More recently, Steppert et al. observed the presence of a trimeric $[(UO_2)_3(OH)_2(CO_3)]^{2+}$ complex, but they suspected that is was caused by the combination of a dimeric $[(UO_2)_2(OH)_2]^{2+}$ and $[(UO_2)(CO_3)]^0$ species because the neutral species could not be observed by the ESI-MS technique.[37]

Most speciation studies are performed in dilute solutions ($[U^{6+}] = 10^{-5}$ M) to prevent the formation of uranyl colloids, whereas crystallization studies are performed under more concentrated solutions that could result in the formation of different molecular species. The formation of the larger molecular species in **3** may only occur at higher uranyl concentrations in solution but could be composed of building units present in more dilute solutions. The 3:2 uranyl malic trimeric units have also been proposed based upon potentiometric studies, and the individual building blocks of the pentameric species, namely, the 2:1 uranyl malate dimer $[(UO_2)_2(OH)(mal)(H_2O)_4]^0$ and the uranyl carbonate monomer $[(UO_2)(CO_3)_2]^{2-}$, are also expected to exist in solution.[29,36a] Additional solution-based studies, such as EXAFS or HEXS spectroscopy, are necessary to provide a better understanding for the conditions that favor individual dimeric and trimeric species over the larger hydrolysis products.

CONCLUSIONS

The synthesis and structural characterization of three novel molecular compounds extend our structural knowledge of the hydrolysis of U^{6+} in the presence of organic ligands at near-neutral pH regions. Isolation of a novel uranyl trimer observed in compound **1** illustrates the interplay between hydrolysis and chelation by organic ligands and the importance of structural characterization to aid in the interpretation of spectroscopic data. The structural nature of the 3:3 malic trimer is confirmed in compound **2**, and a trimeric and pentameric species link through hydroxyl bridges and carbonate anions to form the larger polynuclear array observed in compound **3**. A greater understanding of the interaction of organic species with the uranyl cation in solution is essential both for better speciation modeling in aqueous systems and for targeting the molecular building units that are the basis of hybrid organic−inorganic materials. Continued crystallization of the molecular species combined with spectroscopic characterization is necessary to thoroughly characterize and understand these highly complex systems.

ASSOCIATED CONTENT

Supporting Information

CIF files, powder X-ray diffraction patterns, and TGA analysis are available in the Supporting Information. This material is available free of charge via the Internet at http://pubs.acs.org.

AUTHOR INFORMATION

Corresponding Author

*E-mail: tori-forbes@uiowa.edu. Fax: 319-335-1270. Tel.: 319-384-1320.

Notes

The authors declare no competing financial interest.

ACKNOWLEDGMENTS

This work was supported by the Nuclear Regulatory Commission Faculty Development Grant NRC-HQ-12-G-38-0041 and the University of Iowa College of Liberal Arts and Sciences. We also thank Professor Peter C. Burns, Director of the Actinide Materials EFRC at the University of Notre Dame, for use of the SensIR instrument and Professor Edward Gillan for the Nicolet FTIR. We thank the UI Central Microscopy Facility for use of the Raman spectrometer and Drs. Santhana Velupillai and Fu Chen of the UI NMR Facility for collection of the MAS NMR spectra.

REFERENCES

(1) Baes, C. F.; Mesmer, R. E. *The Hydrolysis of Cations*; John Wiley and Sons: New York, NY, 1976.
(2) (a) Knope, K. E.; Soderholm, L. *Chem. Rev.* **2013**, *113*, 944−994. (b) Walther, C.; Denecke, M. A. *Chem. Rev.* **2013**, *113*, 995−1015.
(3) (a) Schmidt, M.; Wilson, R. E.; Lee, S. S.; Soderholm, L.; Fenter, P. *Langmuir* **2012**, *28*, 2620−2627. (b) Powell, B. A.; Dai, Z.; Zavarin, M.; Zhao, P.; Kersting, A. B. *Environ. Sci. Technol.* **2011**, *45*, 2698−2703. (c) Soderholm, L.; Almond, P. M.; Skanthakumar, S.; Wilson, R. E.; Burns, P. C. *Angew. Chem., Int. Ed.* **2008**, *47*, 298−302. (d) Kersting, A. B. *Inorg. Chem.* **2013**, *52*, 3533−3546. (e) Maher, K.; Bargar, J. R.; Brown, G. E. *Inorg. Chem.* **2013**, *52*, 3510−3532.
(4) Biswas, B.; Mougel, V.; Pecaut, J.; Mazzanti, M. *Angew. Chem., Int. Ed.* **2011**, *50*, 5744−5747.
(5) Tsushima, S.; Rossberg, A.; Ikeda, A.; Mueller, K.; Scheinost, A. C. *Inorg. Chem.* **2007**, *46*, 10819−10826.
(6) (a) Thuery, P.; Nierlich, M.; Souley, B.; Asfari, Z.; Vicens, J. *J. Chem. Soc., Dalton Trans.* **1999**, *15*, 2589−2594. (b) Zheng, Y. Z.; Tong, M. L.; Chen, X. M. *Eur. J. Inorg. Chem.* **2005**, *20*, 4109−4117. (c) Burns, P. C. *Can. Mineral.* **2001**, *39*, 1139−1146. (d) Mihalcea, I.; Henry, N.; Clavier, N.; Dacheux, N.; Loiseau, T. *Inorg. Chem.* **2011**, *50*, 6243−6249. (e) Alsobrook, A. N.; Hauser, B. G.; Hupp, J. T.; Aekseev, E. V.; Depmeier, W.; Albrecht-Schmitt, T. E. *Cryst. Growth Des.* **2011**, *11*, 1385−1393.
(7) Rowland, C. E.; Cahill, C. L. *Inorg. Chem.* **2010**, *49*, 6716−6724.
(8) Moulin, V.; Tits, J.; Ouzounian, G. *Radiochim. Acta* **1992**, *58/59*, 179−190.
(9) Hoft, R. W. W. *COLLECT*; Nonius, B.V.: Delft, The Netherlands, 1998.
(10) Sheldrick, G. M. *APEX II*, Bruker AXS: Madison, WI, 1996.
(11) Sheldrick, G. M. *Acta Crystallogr., Sect. A: Found. Crystallogr.* **2008**, *64*, 112−122.
(12) Spek, A. L. *PLATON, A Multipurpose Crystallographic Tool*; Utrecht University: Utrecht, The Netherlands, 2005.
(13) Aberg, M. *Acta Chem. Scand., Ser. A* **1978**, *32*, 101−107.
(14) Rowland, C. E.; Cahill, C. L. *Inorg. Chem.* **2010**, *49*, 8668−8673.
(15) Sun, D.; Zhang, N.; Xu, Q.-J.; Huang, R.-B.; Zheng, L.-S. *Inorg. Chem. Commun.* **2010**, *13*, 859−862.
(16) Salmon, L.; Thuery, P.; Ephritikhine, M. *Polyhedron* **2004**, *23*, 623−627.
(17) Burns, P. C. *Can. Mineral.* **2005**, *43*, 1839−1894.
(18) Demartin, F.; Diella, V.; Donzelli, S.; Gramaccioli, C. M.; Pilati, T. *Acta Crystallogr., Sect. B: Struct. Sci.* **1991**, *47*, 439−446.
(19) Hughes, K. A.; Burns, P. C. *Am. Mineral.* **2003**, *88*, 962−966.
(20) Qiu, J.; Burns, P. C. *Chem. Rev.* **2013**, *113*, 1097−1120.
(21) Sigmon, G. E.; Unruh, D. K.; Ling, J.; Weaver, B.; Ward, M.; Pressprich, L.; Simonetti, A.; Burns, P. C. *Angew. Chem., Int. Ed.* **2009**, *48*, 2737−2740.
(22) (a) Ling, J.; Qiu, J.; Burns, P. C. *Inorg. Chem.* **2012**, *51*, 2403−2408. (b) Ling, J.; Ozga, M.; Stoffer, M.; Burns, P. C. *Dalton Trans.* **2012**, *41*, 7278−7284. (c) Ling, J.; Qiu, J.; Sigmon, G. E.; Ward, M.; Szymanowski, J. E. S.; Burns, P. C. *J. Am. Chem. Soc.* **2010**, *132*, 13395−13402. (d) Ling, J.; Wallace, C. M.; Szymanowski, J. E. S.; Burns, P. C. *Angew. Chem., Int. Ed.* **2010**, *49*, 7271−7273.

(23) Cejka, J. Infrared Spectroscopy and Thermal Analysis of the Uranyl Minerals. In *Uranium: Mineralogy, Geochemistry, and the Environment*; Burns, P. C., Finch, R. J., Eds.; Mineralogical Society of America: Washington, D.C., 1999.
(24) Krishnamurthy, M.; Morris, K. B. *Inorg. Chem.* **1969**, *8*, 2620−2624.
(25) Fortier, S.; Hayton, T. W. *Coord. Chem. Rev.* **2010**, *254*, 197−214.
(26) Baranska, H.; Kuduk-Jaworska, J.; Szostak, R.; Romaniewska, A. *J. Raman Spectrosc.* **2003**, *34*, 68−76.
(27) Jiang, J.; Sarsfield, M. J.; Renshaw, J. C.; Livens, F. R.; Collison, D.; Charnock, J. M.; Helliwell, M.; Eccles, H. *Inorg. Chem.* **2002**, *41*, 2799−2806.
(28) Chen, M.-L.; Gao, S.; Zhou, Z.-H. *Dalton Trans.* **2012**, *41*, 1202−1209.
(29) Kakihana, M.; Nagumo, T.; Okamoto, M.; Kakihana, H. C. *J. Phys. Chem.* **1987**, *91*, 6128−6136.
(30) Papenguth, H. W.; Kirkpatrick, R. J.; Montez, B.; Sandberg, P. A. *Am. Mineral.* **1989**, *74*, 1152−1158.
(31) (a) Jiang, J.; Renshaw, J. C.; Sarsfield, M. J.; Livens, F. R.; Collison, D.; Charnock, J. M.; Eccles, H. *Inorg. Chem.* **2003**, *42*, 1233−1240. (b) Dibernardo, P.; Tomat, G.; Bismondo, A.; Traverso, O.; Magon, L. *J. Chem. Res.* **1980**, *7*, 234−235.
(32) (a) Leciejewicz, J.; Alcock, N. W.; Kemp, T. J. *Coord. Chem.* **1995**, *82*, 43−84. (b) Tian, G.; Rao, L.; Teat, S. J.; Liu, G. *Chem.—Eur. J.* **2009**, *15*, 4172−4181. (c) Rao, L. F.; Garnov, A. Y.; Jiang, J.; Di Bernardo, P.; Zanonato, P.; Bismondo, A. *Inorg. Chem.* **2003**, *42*, 3685−3692. (d) Lennartson, A.; Hakansson, M. *Acta Crystallogr., Sect. C: Cryst. Struct. Commun.* **2010**, *66*, M69−M74.
(33) (a) Battiston, G.; Sbrignadello, G.; Bandoli, G.; Clemente, D. A.; Tomat, G. *J. Chem. Soc., Dalton Trans.* **1979**, *12*, 1965−1971. (b) Bombieri, G.; Croatto, U.; Graziani, R.; Forselli., E.; Magon, L. *Acta Crystallogr., Sect. B: Struct. Sci.* **1974**, *30*, 407−411.
(34) Rajan, K. S.; Martell, A. E. *J. Inorg. Nucl. Chem.* **1964**, *26*, 1927−1944.
(35) (a) Feldman, I.; Havill, J. R.; Neuman, W. F. *J. Am. Chem. Soc.* **1954**, *76*, 4726−4732. (b) Pedrosa, J. D.; Gil, V. M. S. *J. Inorg. Nucl. Chem.* **1974**, *36*, 1803−1807.
(36) (a) Gotz, C.; Geipel, G.; Bernhard, G. *J. Radioanal. Nucl. Chem.* **2011**, *287*, 961−969. (b) Krestou, A.; Panias, D. *Eur. J. Miner. Process. Environ. Prot.* **2004**, *4*, 113−129.
(37) Steppert, M.; Walther, C.; Fuss, M.; Buchner, S. *Rapid Commun. Mass Spectrom.* **2012**, *26*, 583−591.